Tetrahedron Vol. 49, No. 30, pp. 6545-6560, 1993
Printed in Great Britain

0040-4020/93 $6.00+.00

NMR and Molecular Modeling Study of the Conformations of Taxol and of its Side Chain Methylester in Aqueous and Non-Aqueous Solution.

Howard J. Williams, A. Ian Scott*, Reiner A. Dieden

Center for Biological NMR, Department of Chemistry, Texas A&M University, College Station, Texas 77843-3255

Charles S. Swindell*, Lisa E. Chirlian, Michelle M. Francl, Julia M. Heerding, Nancy E. Krauss

Department of Chemistry, Bryn Mawr College, 101 North Merion Avenue, Bryn Mawr, Pennsylvania 19010-2899

(*Received in USA* 3 *May* 1993)

Key Words: Taxol ; Taxol Side Chain Methyl Ester ; Conformation

Abstract: *The conformations of the antimitotic agent taxol and its side chain methyl ester have been studied by NMR-spectroscopy and molecular modeling in hydrophobic ($CDCl_3$) and hydrophilic (water, d_6-DMSO) solvents. For the side chain methly ester (4), the coupling constant $J_{H2'-H3'}$ changes from ~2 Hz in chloroform to ~5 Hz in d_6-DMSO or water : d_6-DMSO, 1 : 1 (v/v). The conformational equilibrium for 4 thus shifts from one favoring conformers with a* gauche *<H-C2'-C3'-H> torsion angle (chloroform), to one predominantly of conformers having this torsion angle* anti. *In the case of taxol, $J_{H2'-H3'}$ changes from 2.7 Hz in $CDCl_3$ to ~8 Hz in water, water - sodium dodecyl sulfate (SDS) and/or d_6-DMSO. Again, gauche conformations are implicated in chloroform, but molecular modeling suggests the* anti *conformer 27 to be dominant in aqueous media and in d_6-DMSO. No nuclear Overhauser effects (nOe's) between the side chain and the taxane ring-system are observed in chloroform solution. In water and/or d_6-DMSO, however, nOe's between the side chain (Ph3' and H2') and the OAc4 methyl group are detected.*

Taxol[1] **1**, a diterpenoid natural product of the Pacific yew (*Taxus brevifolia* Nutt.) and related yew species, is rapidly developing into the most important antitumor chemotherapeutic agent to reach clinical application in some time. Highly encouraging phase II activities against drug refractory ovarian[2] and breast[3] carcinomas have been observed. Taxol is not only structurally unusual among cytotoxic drugs, but operates through a unique mechanism at the cellular level whereby it binds to microtubules, promotes their assembly from tubulin heterodimers, and stabilizes them against depolymerization. Classical anti-mitotic substances such as vinblastine and colchicine affect the tubulin-microtubule system in essentially the opposite way. The resulting abnormal tubulin-microtubule equilibrium disrupts the normal mitotic spindle apparatus, which underlies the ability of taxol to block cell proliferation at the tetraploid G_2-M phases of the cell cycle.[4] Thus, taxol offers new structural and mode-of-action leads that promise to form the basis of a distinct class of antineoplastic drugs, which now includes the taxol analogs Taxotere®,[5] **2** and cephalomannine **3**.

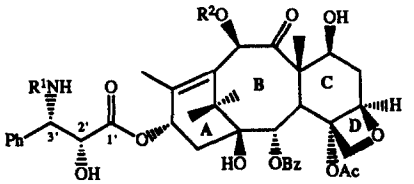

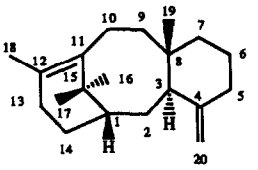

1 R^1 = Bz; R^2 = Ac Taxol
2 R^1 = t-BuO_2; R^2 = H Taxotere®
3 R^1 = tigloyl; R^2 = Ac Cephalomannine

One aim of current chemical research in this area is the determination of the structural features of the apparently non-covalent[4] taxol-microtubule interaction. This recognition phenomenon might then be rationally exploited in the subsequent design of next-generation drugs. Photoaffinity labeling studies have indicated that the tubulin β chain plays a major role in the taxol binding regions,[6] although much work remains before a detailed picture will emerge of the elements of tubulin and microtubules that are involved in taxol binding. Another component of this problem is the definition of the bound conformations of taxol, an effort that might sensibly be preceded by the determination of its unbound conformations of taxol in hydrophilic and hydrophobic media.[7] A model compound study for ring A side chain was included because most conformational changes occur in this non-rigid portion of the molecule, models were necessary for conformer elucidation, and preliminary structure-activity correlation studies indicate that subtle changes in side chain functionality or stereochemistry profoundly affect activity.[4]

Apart from recent NMR investigations[8] of taxol in hydrophobic media that have provided data relevant to the solution conformations of taxol, detailed structural information has been restricted to the X-ray crystallographic structures of Taxotere,®[9] of the taxol A-ring side chain methyl ester **4**,[10] and of the cephalomanine A-ring side chain methyl ester.[11] An X-ray crystallographic structure for taxol itself

remains unavailable. In an attempt to fill this gap, we wish to report ^{1}H-NMR and molecular modeling studies of taxol and its A-ring side chain methyl ester **4** in a series of aqueous and non-aqueous solvent systems that lead to important conclusions regarding their conformational preferences.

EXPERIMENTAL

Source of chemicals studied. Taxol was obtained from Dr. Matthew Suffness, National Cancer Institute, National Institutes of Health. A combination of the Greene[12b] and Jacobsen[12f] procedures was employed for the preparation of **4**.[12] Model compounds N-benzyl benzamide **5**, 1-(N-benzoyl-2-aminobutyl)benzoate **6** and 1-N-benzoyl-2-aminobutanol **7** were prepared from benzoyl chloride and the corresponding amines[13] and purified by thin layer chromatography. For convenience and in order to simplify the comparison of the NMR-parameters, the same numbering system as for the taxol side chain was used for compounds **4** - **7**.

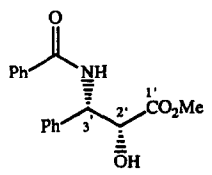

4

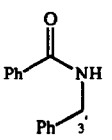

5

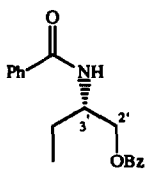

6

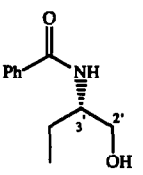

7

NMR studies. ^{1}H-NMR spectroscopy was performed either at 500 MHz on a Varian Unity 500 equipped with a Sun data system or a Bruker AM-500 with ASPECT 3000 data system, or at 300 MHz on a Bruker WM-300 spectrometer with ASPECT 2000 data system. Spectra were taken at room-temperature unless stated otherwise. ^{1}H-chemical shifts are referenced relative to the solvent peak, i.e. chloroform for the $CDCl_3$-sample ($\delta(CHCl_3)$ = 7.24 ppm), water for the SDS-sample (δ(HDO) = 4.63 ppm), dimethylsulfoxide for all DMSO-containing samples ($\delta(d_5\text{-DMSO})$ = 2.49 ppm).

1D-Spectra were taken with 32k data points (0.2 Hz/point), while the 2D-experiments were performed with matrix-sizes of 1k x 1k (COSY) or 2k x 2k (NOESY). NOESY mixing times were 600, 800 and 1000 msec.

Choice of Solvents. One of the major inconveniences for both clinical and spectroscopic studies of taxol is its virtually complete lack of solubility in the most interesting solvent for such purposes, water. Solubility can be substantially enhanced, however, through addition of either perdeutero sodium dodecyl sulfate (d_{25}-SDS) or hexadeuterodimethylsulfoxide (d_6-DMSO). We find that a mixture of d_6-DMSO : D_2O, 1 : 1 (v/v) is the lower limit for dissolving sufficient material (~500 µg) to obtain the necessary sensitivity for 2D-NMR experiments. Use of 60% and 70% d_6-DMSO further increases the solubility and allows conclusions to be drawn on the effects of the two solvents on conformation. Non-aqueous solvents used are d_6-DMSO and $CDCl_3$, in both of which taxol and **4** are readily soluble.

Molecular modeling. Internal coordinate Monte Carlo conformational searching[14] was carried out on a Silicon Graphics 4D/35 workstation using MacroModel[15] (version 3.1) with the included version of the MM2 force field[16] and the Still chloroform and water continuum solvation models[17] (as indicated below). The inspection and analysis of the conformational data were facilitated by the use of SYBYL (version 5.5). All taxane starting structures were generated from the Taxotere® crystal structure coordinates.[9]

The treatment of the taxol side chain methyl ester was straightforward and used the default MacroModel search parameters. Since complete searches of conformational space are impossible given the currently available technology, it is necessary to evaluate the search results to ensure that the resulting conformations are representative of the low energy conformations available to the structure examined. This is generally accomplished by determining the number of times the lower energy structures are found during the search. For the side chain methyl ester, adequate redundancy was accomplished easily using 1000 initial structures as specified in the MacroModel default parameters. Preliminary conformational searches for the complete taxol structure indicated that a fully unconstrained search would be prohibitively time-consuming. Therefore, an unconstrained search (without solvation) of 13-acetyl baccatin III (acetyl group instead of the A-ring side chain acyl group in the taxol structure) was performed to gauge the flexibility of the carbon skeleton. No conformations that differed significantly from the global minimum were found within several kcal·mol^{-1}. Subsequent searches for the complete taxol structure were carried out with variable torsion angles in the A-ring side chain, the OAc4 group, and in the C-ring to account for the possibility of oxetane-induced half-chair flexibility. The A and B-rings were not explicitly varied (in the determination of new conformations) but were allowed to relax during the subsequent energy minimizations, as were the remaining side chains on the B and C-rings.

The conformational searches produced large numbers of conformations, many of which were closely related (differing only by rotations of the 3'-phenyl ring, for example). The examination of the search results, as well as chemical intuition, indicated that the key side chain torsion angles about C3'-C2', C2'-C1' and O-C13 were responsible for the overall relationship of the side chain to the remainder of the taxol structure. To divide the results into manageable sets, the unique low energy structures were used as templates and higher energy structures were assigned to a "cluster" based on the similarity of their key torsion angles to those of a particular low energy template. This was justified by the relatively narrow ranges within which these torsion angles fell. A clustering range of ±60° was found to be the most convenient, yielding sets of structures that had the same overall characteristics but excluding those that were grossly different. Smaller ranges gave more sets of structures, however many had essentially identical torsional characteristics. This procedure yielded for taxol side chain methyl ester **4** six chloroform solvation (**8-13**) and six water solvation (**14-19**) fundamental conformational types and for taxol **1** five chloroform solvation (**20-24**) and four water solvation (**25-28**) fundamental conformational types within 2 kcal·mol^{-1} of the respective global minima.[18] Since molecular mechanics methods are not expected to make fine energetic distinctions among conformers, the relative energies or these trial structures are not highly significant.

RESULTS

The Taxol A-Ring Side Chain Methyl Ester (4)

As a first step towards the conformational study of taxol, the ^{1}H-NMR spectra of the taxol side chain methyl ester **4** were recorded for data comparison. The ^{1}H chemical shifts and coupling constants in deuterochloroform, water - d_6-DMSO, 1 : 1 (v/v) and d_6-DMSO are reported in Tables 1 and 2, respectively.

The data most relevant for discussion of conformation are the coupling constants $J_{H2'-H3'}$ and $J_{H3'-NH}$. Inspection of Table 2 shows that the latter is essentially independent of the solvent, having a value of ~9 Hz in each of the solvents studied. The coupling constant between H2' and H3', however, doubles its value on passing from $CDCl_3$ ($J_{H2'-H3'}$ = 2.1 Hz) to water - d_6-DMSO, 1 : 1 (v/v) or d_6-DMSO ($J_{H2'-H3'}$ = 4.7 Hz or 5.5 Hz).

Table 1. ^{1}H NMR Chemical Shifts for the Taxol Side Chain Methyl Ester **4** in Deuterochloroform and Water - d_6-DMSO, 5 : 5 (v/v) and d_6-DMSO (δ ; ppm).

	$CDCl_3$	DMSO[a] 50%	DMSO 100%
H2'	4.58	[b](4.52)[c,d]	4.48
H3'	5.68	5.39	5.41
NH	6.95	5.40[c]	8.69
o-Ph-3'	7.39	7.3	7.39
m-Ph-3'	7.31	7.3	7.32
p-Ph-3'	7.24	7.2	7.24
o-NHBz	7.71	7.69	7.83
m-NHBz	7.38	7.44	7.54
p-NHBz	7.45	7.51	7.48
OH2'	[e]	-	5.83
OCH3	3.78	3.51	3.51

[a] in D_2O.
[b] buried under solvent peak.
[c] in H_2O.
[d] at -20°C.
[e] not observed.
[f] small (< 1.5 Hz)

Table 2. ^{1}H-^{1}H Coupling Constants for the Taxol Side Chain Methyl Ester **4** in Deuterochloroform, Water - d_6-DMSO, 5 : 5 (v/v) and d_6-DMSO (J ; Hz).

	$CDCl_3$	DMSO[a] 50%	DMSO 100%
H2'-H3'	2.1	4.7	5.5
H3'-NH	9.1	8.8[c]	8.8
o-mPh	7.3	7.3	7.6
o-pPh	1.4	1.4	1.5
m-pPh	8.1	8.1	7.2
o-mNHBz	7.0	7.4	7.1
o-pNHBz	1.5	[f]	1.4
m-pNHBz	7.4	7.5	7.2
2'-OH2'	[e]	7.7	[e]

Regardless of the solvation treatment employed, molecular modeling identifies the same low energy conformational types for this structure. These are summarized in Tables 3 and 4. There appear computationally to be no very well defined torsional preferences about the N-C3' bond, an observation that may be related to the apparently rotationally-averaged $J_{NH-H3'}$ values detected regardless solvent.

Table 3. Chloroform Conformational Types for **4**.

conformer	<N-C3'-C2'-O> [deg]	<O-C2'-C1'=O> [deg]	calcd.[a] $J_{H2'-H3'}$ [Hz]	relative energy [kcal·mol^{-1}]
8	-63	-7	1.2	0
9	-83	164	2.5	0.1
10	178	175	4.2	0.6
11	49	-172	10.6	1.2
12	177	-5	4.1	1.2
13	48	30	10.6	1.3

[a] The couplings constants were calculated with the Karplus relationship implemented in MacroModel.

Table 4. Water Conformational Types for **4**.

conformer	<N-C3'-C2'-O> [deg]	<O-C2'-C1'=O> [deg]	calcd. $J_{H2'-H3'}$ [Hz]	relative energy [kcal·mol^{-1}]
14	-67	-2	1.6	0
15	56	12	10.4	0.4
16	176	-177	3.9	0.5
17	177	3	4.2	0.5
18	-64	-171	1.2	0.9
19	53	-167	10.6	2.0

[a] The couplings constants were calculated with the Karplus relationship implemented in MacroModel.

This conclusion is confirmed by the values of $J_{NH-H3'}$ observed for three model compounds (**5**, **6**, and **7**), for which it is reasonably safe to assume free rotation around the N-C3' bond (Table 5). The low value observed for N-benzyl benzamide **5** (5.6 Hz) is due to the absence of the electronegative substituent. In **6** and **7**, the $J_{NH-H3'}$ values are increased to 8.3 and 8.1 Hz, respectively. These values are in reasonable agreement with the 9 Hz observed for **4**, especially since the presence of the supplementary methoxycarbonyl group is likely to further increase the coupling constant in the latter and in taxol.

Table 5. $J_{NH-H3'}$ data for compounds **5**, **6** and **7** in $CDCl_3$ (Hz).

compound	**5**	**6**	**7**
$J_{NH-H3'}$	5.6	8.3	8.1

In chloroform, the small 2.1 Hz $J_{H2'-H3'}$ value allows conformational types **11** and **13** with large <H-C2'-C3'-H> torsion angles to be rejected. Chloroform solvation search global minimum **8** has essentially the same conformational characteristics as the Taxotere,® taxol side chain methyl ester **4**, and cephalomanine side chain methyl ester X-ray crystallographic structures. Indeed, the simplest description of the chloroform solution structure of **4** consistent with the computational and NMR evidence is that conformer **8** is the major contributor. Conformer **8** is organized by a hydrogen bond between the OH2' and the ester carbonyl oxygen, and one between the NH and OH2' oxygen. An independent study of **4** in chloroform solution employing vibrational circular dichroism (VCD), a technique sensitive to chiral environments near hydrogen bonds and operative over a shorter spectroscopic time scale (thus sensitive to torsion about N-C3'), has arrived at this conclusion.[19]

In aqueous and neat d_6-DMSO, the full range of conformational types **14** - **19**, including <H-C2'-C3'-H> *anti* conformations like **15**, is allowed by the larger values of ~5 Hz observed for $J_{H2'-H3'}$, and the inability of the NMR data to provide information on torsion about the C1'-C2' bond. Again, a conformation essentially equivalent to that observed in the X-ray crystallographic studies appears as the global minimum (**14**) in the water solvation search for **4**.

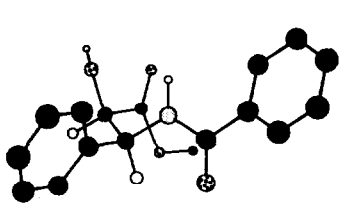

8

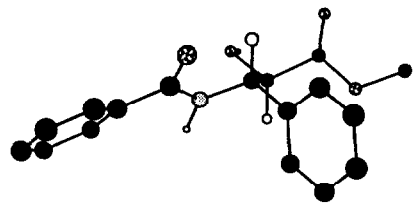

15

Taxol

The chemical shift data and coupling constants for taxol in the different solvent systems are assembled in Tables 6 and 7, respectively.

Deuterochloroform. Our assignments in this solvent are in complete agreement with an earlier report.[8a] The three most deshielded signals, beside those of the aromatic moieties, are the NH doublet at 6.91 ppm, the H10 singlet at 6.20 ppm and the H13 triplet at 6.17 ppm.

Connectivities are easily established from the COSY-spectra. The amide proton NH is coupled to H3' (5.72 ppm, J = 8.9 Hz) which also shows a correlation to H2' (4.73 ppm, J = 2.7 ppm). H13 exhibits couplings to both of the H14 protons (2.32 and 2.25 ppm), as well as to the methyl-protons Me18 (1.77 ppm).

Table 6. ^1H NMR Chemical Shifts for Taxol in Different Solvent Systems (δ ; ppm).

	$CDCl_3$	SDS[a] 40 equ.	DMSO[a] 50%	DMSO[a] 60%	DMSO[a] 70%	DMSO 100%
H2	5.61	5.48	5.36	5.36	5.36	5.40
H3	3.73	3.59	3.52	3.53	3.55	3.60
H5	4.88	4.74	4.94	4.91	4.88	4.91
$H6_\alpha$	2.49	2.29	2.40	2.34	2.30	2.31
$H6_\beta$	1.82	1.74	1.70	1.44	1.60	1.62
H7	4.34	4.15	4.24	4.40	4.05	4.05
H10	6.20	6.28	6.20	6.20	6.21	6.28
H13	6.17	5.95	5.84	5.85	5.83	5.87
$H14_\alpha$	2.32	1.74	1.76	1.81	1.80	1.88
$H14_\beta$	2.25	1.53	1.51	1.57	1.58	1.58
Me16	1.12	0.99	0.95	0.95	0.96	1.01
Me17	1.23	1.05	0.95	0.95	0.96	1.00
Me18	1.77	1.62	1.69	1.70	1.72	1.78
Me19	1.66	1.42	1.44	1.44	1.44	1.49
$H20_\alpha$	4.25	3.54	4.01	4.01	3.96	4.02
$H20_\beta$	4.13	3.44	4.01	4.01	3.96	3.98
OAc4	2.33	2.09	2.16	2.16	2.16	2.22
OAc10	2.18	2.06	2.06	2.08	2.06	2.10
o-Bz2	8.07	7.88	7.89	7.90	7.91	7.96
m-Bz2	7.45	7.34	7.56	7.59	7.59	7.62
p-Bz2	7.65	7.38	7.66	7.68	7.68	7.71
H2′	4.73	[b]	[b]	4.57	4.53	4.57
H3′	5.72	5.36	5.32	5.26	5.30	5.39
NH	6.91	-	6.65[c]	-	-	8.91
o-Ph3′	7.42	7.28	(7.32)	7.35	7.34	7.38
m-Ph3′	7.34	7.17	(7.34)	7.35	7.34	7.39
p-Ph3′	7.29	6.92	7.14	7.14	7.15	7.21
o-NHBz	7.68	7.73	7.71	7.75	7.79	7.81
m-NHBz	7.33	7.28	7.41	7.45	7.44	7.48
p-NHBz	7.47	7.37	7.49	7.52	7.52	7.54
OH1	[e]	-	-	-	-	4.70
OH7	[e]	-	-	-	-	[e]
OH2′	[e]	-	-	-	-	6.17

a. in D_2O.
b. buried under solvent peak.
c. in H_2O.
d. small (<1.5 Hz)
e. not observed
f. not determined

Table 7. ^1H-^1H Coupling Constants for Taxol in Different Solvent Systems (Hz).

	$CDCl_3$	SDS[a] 40 equ.	DMSO[a] 50%	DMSO[a] 60%	DMSO[a] 70%	DMSO 100%
H2-H3	7.2	5.6	6.8	7.3	6.3	7.2
$H3\text{-}H20_\alpha$	1.0	-	-	-	-	-
$H5\text{-}H6_\alpha$	9.7	-	9.3	9.5	8.4	8.6
$H5\text{-}H6_\beta$	2.3	-	-	[d]	-	-
$H6_\alpha\text{-}H6_\beta$	14.7	[f]	n	n	n	n
$H6_\alpha$-H7	6.8	n	-	n	-	-
$H6_\beta$-H7	11.2	-	-	n	n	10.7
$H13\text{-}H14_\alpha$	8.9	8.1	8.8	9.5	8.9	8.9
$H13\text{-}H14_\beta$	9.1	9.6	8.8	9.5	8.9	8.9
H13-H18	1.6	-	-	s	s	1.3
$H14a\text{-}H14_\beta$	15.5	-	15.5	15.5	n	15.5
$20_\alpha\text{-}20_\beta$	8.3	11.7	-	-	-	8.3
o-mOBz	8.5	8.4	8.0	8.4	7.8	8.4
o-pOBz	1.3	1.4	s	1.4	s	1.2
m-pOBz	7.5	7.2	7.0	7.6	7.3	7.4
H2′-H3	2.7	8.5	7.3	7.7	7.9	7.8
H2′-OH2′	-	-	-	-	-	7.8
H3′-NH	8.9	-	[8.0][c]	-	-	7.8
H3′-o-Ph	s	-	-	-	-	-
o-mPh	7.7	8.3	n	8.0	n	n
o-pPh	1.6	1.4	s	1.5	s	s
m-pPh	7.2	7.4	6.6	6.6	n	5.3
o-mNHBz	8.3	7.4	8.0	8.2	7.8	8.3
o-pNHBz	1.4	1.4	s	1.2	s	1.3
m-pNHBz	7.0	6.9	7.5	7.4	7.6	7.3

The mutually coupled doublets at 5.61 and 3.73 ppm are attributed to H2 and H3, respectively. Correlations to both the two H6 (2.53 and 1.86 ppm) and the two H20 protons (4.25 and 4.13 ppm) identify the signal at 4.88 ppm as H5. The correlation of H6 establishes H7 at 4.34 ppm.

The methyl groups (Me16, Me17, Me18 and Me19) could be assigned through their nOe interactions (Figure 1) : the phase sensitive NOESY and ROESY spectra show cross-peaks between H13 and Me17 (1.23 ppm), while Me16 is identified as the peak at 1.12 ppm through its nOe with H2. The protons giving rise to a signal at 1.23 and 1.77 ppm are near H13 and H10, identifying them as Me17 and Me18, respectively. Finally, Me19 at 1.99 ppm is identified through its dipolar coupling with H2 and H5. The acetate groups OAc4 and OAc10 have been previously assigned[8a] unequivocally using HMBC.

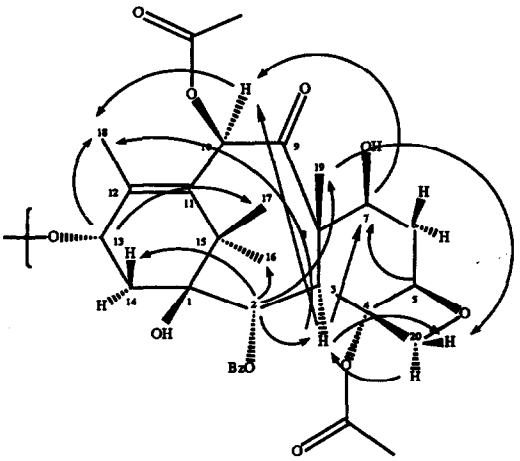

Figure 1. Principal nOe's for taxol **1** in $CDCl_3$.

d_6-Dimethylsulfoxide. Again, the different signals can be easily assigned with the help of COSY and NOESY spectroscopy. The amide NH is the most deshielded proton in the spectrum (8.91 ppm). The network of correlations from NH to H3' (5.29 ppm), from H3' to H2' (4.57 ppm) and from the latter to the hydroxyl-proton OH2' at 6.17 ppm clearly establishes their identities. The characteristic triplet of H13 at 5.87 ppm shows correlations to the two mutually coupled H14 protons (1.88 and 1.58 ppm), as well as to Me18 (1.78 ppm). H5 is coupled to H7 (4.05 ppm) and H6$_\alpha$ (2.31 ppm). The strong correlation between H6$_\alpha$ and H6$_\beta$, as well as the one between H7 and H6$_\beta$, locate the latter at 1.62 ppm.

These assignments are corroborated and completed by the NOESY-data. H13 and H2 show nOe's with the bridgehead methyl groups Me16 and Me17, which are located almost as a single line at 1.01 and 1.00 ppm. The signal of those two methyl groups shows a cross-peak with a sharp singlet at 4.70 ppm, identifying it as the OH1 proton.

NOESY-correlations with H7, H3 and Me18 establish the 6.28 ppm-singlet as H10. The Me19 methyl protons could be located at 1.49 ppm, as revealed by their dipolar coupling to H2. They show a further correlation with the tight AB-system of the H20 hydrogens (4.02 and 3.98 ppm).

More interesting, however, are nOe-interactions between some of the side chain protons and the ring system (Figure 2). In fact, while H3' shows a cross-peak to the signal of the (undifferentiated) *ortho*- and *meta*-protons of the 3'-phenyl moiety, it also exhibits a nOe correlation with H3. Furthermore, both the H2' and the *o*- and *m*-Ph-protons are correlated to the acetate-CH_3 at 2.25 ppm, establishing it as OAc4,[20] leaving the signal at 2.10 ppm to be assigned to OAc10.

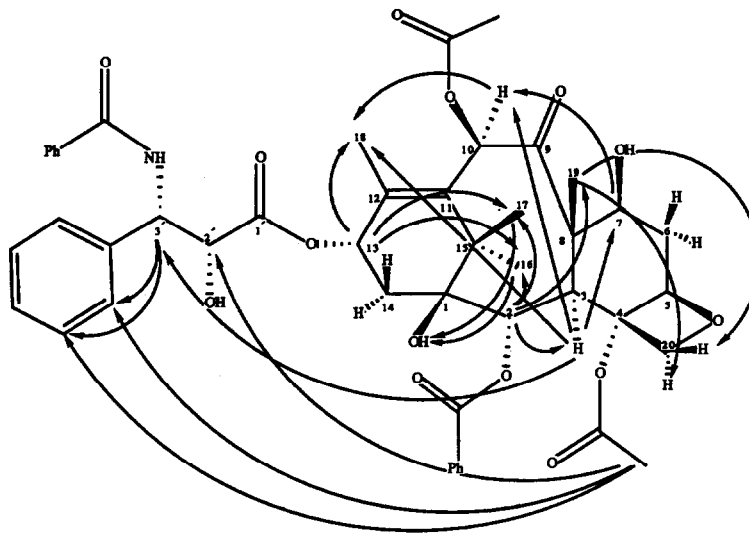

Figure 2. Principal nOe's for taxol **1** in d_6-DMSO.

DMSO-water mixtures. Assignment of the different peaks was achieved in an analogous manner to the DMSO-sample, the spectra being essentially identical. Inspection of Table 6 indicates that the chemical shifts of the different protons are, with the exceptions of the exchanging ones (OH, NH), only very slightly variant with the DMSO-water ratio and are essentially identical to those observed in pure d_6-DMSO solution.

It is especially noteworthy that the side chain coupling constants also appear to be almost invariant in those solvent-systems ($7.3 \leq J_{H2'-H3'} \leq 7.9$; $8.0 \leq J_{NH-H3'} \leq 8.5$), suggesting that the conformation should be very similar. Therefore, based on the J data, taxol in d_6-DMSO seems to be a good model for taxol in water. This is corroborated by the fact that we observe a nuclear Overhauser effect between the *o*- and/or *m*-Ph protons and the acetyl group OAc4, at least in the d_6-DMSO-D_2O, 7 : 3 (v/v) sample.

SDS-micelles. In this solvent system also, no very important chemical shift changes relative to those observed in DMSO-solution were observed. Assignments follow the same pattern as previously and are straightforward.

The NOESY-spectra display nuclear Overhauser effects similar to those observed for the other aqueous solutions. H10 (6.28 ppm) interacts with the Me18 methyl protons (1.75 ppm). H13 shows a NOESY-crosspeak with the bridgehead-methyl Me17, while H2 is correlated with both Me16 and Me19. Here, too, we observe a nuclear Overhauser effect between the acetate group OAc4 at 2.09 ppm and the *o*- and/or *m*-phenyl protons at 7.38 ppm.

Molecular Modelling. Computational investigation of the complete taxol structure reveals greater energetic differences among the side chain conformational types. Thus, subsets of the above side chain methyl ester conformational categories are found in the lowest 2 kcal·mol^{-1} ranges of the chloroform and water conformer ensembles. These are summarized in Tables 8 and 9. Again, well defined torsion angles about the N-C3' bond are neither apparent computationally, nor obvious from the $J_{NH-H3'}$ data.

Table 8. Chloroform Conformational Types for Taxol.

conformer	<N-C3'-C2'-O> [deg]	<O-C2'-C1'=O> [deg]	<C1'-O-C13-C12> [deg]	calcd.[a] $J_{H2'-H3'}$ [Hz]	relative energy [kcal·mol^{-1}]
2 0	-84	-167	-158	2.7	0
2 1	-60	-162	-93	0.9	0.5
2 2	-59	11	-149	1.0	0.9
2 3	178	174	-154	4.1	1.1
2 4	48	177	-162	10.6	1.8

[a] The couplings constants were calculated with the Karplus relationship implemented in MacroModel.

Table 9. Water Conformational Types for Taxol.

conformer	<N-C3'-C2'-O> [deg]	<O-C2'-C1'=O> [deg]	<C1'-O-C13-C12> [deg]	calcd.[a] $J_{H2'-H3'}$ [Hz]	relative energy [kcal·mol^{-1}]
2 5	-62	16	-155	1.3	0
2 6	-62	-164	-92	1.1	0.8
2 7	59	37	-95	10.4	1.4
2 8	-88	-179	-163	3.7	1.6

[a] The couplings constants were calculated with the Karplus relationship implemented in MacroModel.

Among the fundamental chloroform conformers in Table 8, **24**, which has a large <H-C2'-C3'-H> torsion angle, may be eliminated on the basis of the small $J_{H2'-H3'}$ value detected in this solvent. The remaining chloroform conformers are more or less equally consistent with $J_{H2'-H3'}$. Conformer **22** is analogous to the Taxotere® solid state structure, which has recently been proposed[8d] on the basis of time dependent nOe data to be the dominant taxol conformer in chloroform solution. An independent VCD study of taxol in chloroform concurs, but identifies a conformer like **23** as a less populated but significant contributor to the taxol conformational equilibrium in that medium. Conformers **20** and **21** were rejected in the VCD study.[19]

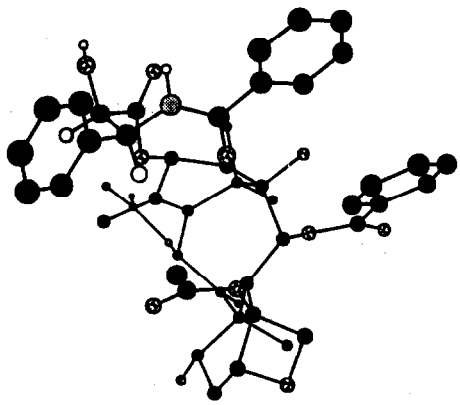

22

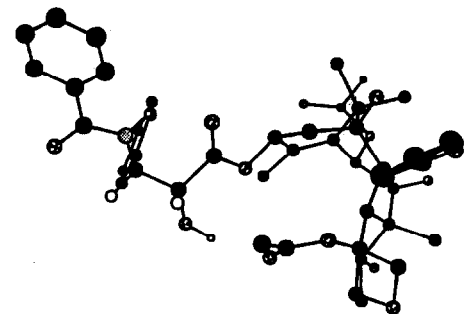

23

The NMR and computational data for taxol in aqueous media are striking. The $J_{H2'-H3'}$ values of ~8 Hz observed in aqueous d_6-DMSO (and neat d_6-DMSO and SDS-micelles) point to the dominant contribution of conformers with large <H-C2'-C3'-H> torsion angles. Furthermore, the computational data reveal that a <H-C2'-C3'-H> torsion angle near 180° (i.e., conformer **27**) is highly correlated among the low energy taxol water conformers with the torsions about C1'-C2' and O-C13 indicated for **27** in Table 9. Together this information specifies conformational type **27** as the dominant one in these media. Conformer **27** is consistent with the nOe's observed for the H2'/OAc4 and Ph3'/OAc4 pairs. Of the remaining low energy conformational types identified by molecular modeling (global minimum **25**, **26** and **28**) that would possess low values for $J_{H2'-H3'}$ and thus might be expected to be minor equilibrium contributors in aqueous medium, **25** and **26** show close contacts betweeen Ph3' and OAc4, and **28** shows a close contact between H2' and OAc4. Conformer **25** is, again, much like the Taxotere® solid state structure.

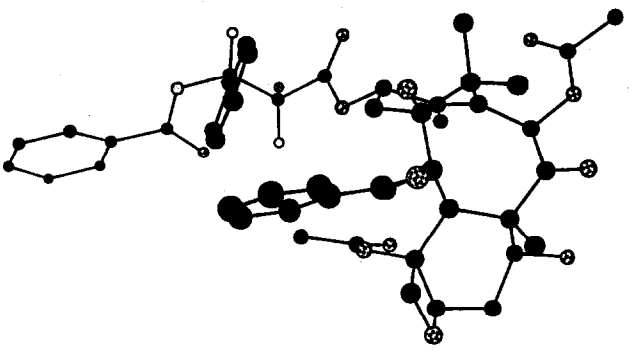

27

DISCUSSION

Changes in taxol conformation due to solvent effects occur mainly in the A-ring side chain, since the diterpenoid portion of the structure is far less flexible. The major conformational changes which the diterpenoid portion undergoes occur in the B ring. For example, $J_{H2\text{-}H3}$ varies from 7.2 Hz in $CDCl_3$, d_6-DMSO, and water-d_6-DMSO to 5.6 Hz in SDS-micelles, indicating a change in the <H-C2-C3-H> torsion angle from approximately 142° to 152°.

Much more substantial solvent-induced conformational changes are observed for the side chain as recorded by the $J_{H2'\text{-}H3'}$ data. The spectrum of taxol in chloroform exhibits a value for this coupling constant of 2.7 Hz. That no nOe's between the side chain and ring system protons are observed in chloroform[20] is qualitatively consistent with the absence of strong interactions between these two moieties in non-globular conformations. In contrast, in aqueous and d_6-DMSO solutions the spectrum is characterized by a $J_{H2'\text{-}H3'}$ of approximately 8 Hz, indicative of a profoundly different side chain conformational ensemble. Furthermore, the nuclear Overhauser effects shown by taxol in these solvents between the *o*- and/or *m*-3'-phenyl protons and OAc4, and H2' and OAc4 implicate conformations in which the side chain and OAc4 - well separated covalently - are spatially proximate in more globular structures. Nevertheless, the two respective major conformations identified - **22** in chloroform and **27** in aqueous medium - cannot be neatly classified in these terms. The most obvious difference between

the two is the greater exposure to solvent of the hydrophobic 3'-phenyl group in chloroform conformer **22**, and the greater exposure of the polar side chain benzamide group in water conformer **27**.

The coupling constants $J_{H2'-H3'}$ in taxol and **4** in chloroform are very similar in magnitude but in aqueous medium and neat d_6-DMSO are divergent (approximately 8 Hz for taxol and 5 Hz for **4**). Evidently in the latter media, the diterpenoid core of taxol discriminates effectively between H2'/H3' *gauche* conformations **25**, **26** and **28**, and H2'/H3' *anti* conformation **27**.

With these data in hand for both hydrophobic and hydrophilic solvent systems, we are now able to probe the conformational perturbation that might obtain when taxol binds to microtubules.

ACKNOWLEDGEMENTS

Support from National Institutes of Health to A.I.S. (GM 32596) and through USPHS Grant No. CA 55139 (C.S.S.) awarded by the National Cancer Institute, DHHS is gratefully acknowledged. N.E.K. thanks the United States Department of Education for a GAANN fellowship and R.A.D. wishes to thank NATO for a fellowship. We are grateful to Dr. Matthew Suffness, National Cancer Institue, National Institutes of Health for providing the taxol sample, and to Dr. J.W. Clader, Schering-Plough Research for his MacroModel-SYBYL interface.

REFERENCES AND NOTES

1. Wani, M.C.; Taylor, H.L.; Wall, M.E.; Coggon, P.; McPhail, A.T. *J. Am. Chem. Soc.* **1971**, *93*, 2325.
2. McGuire, W.P.; Rowinsky, E.K.; Rosenschein, N.B.; Grumbine, F.C.; Ettinger, D.S.; Armstrong, D.K.; Donehower, R.C. *Ann. Intern. Med.* **1989**, *111*, 273.
3. Holmes, F.A.; Walters, R.S.; Theriault, R.L.; Forman, A.D.; Newton, L.K.; Raber, M.N.; Buzdar, A.U.; Frye, D.K.; Hortobagyi, G.N. *J. Natl. Cancer Inst. (Bethesda)* **1991**, *83*, 1797.
4. (a) Schiff, P.B.; Fant, J.; Horwitz, S.B. *Nature*, **1979**, *277*, 665. (b) Schiff, P.B.; Horwitz, S.B. *Proc. Natl. Acad. Sci. USA* **1980**, *77*, 1561. (c) Manfredi, J.J.; Horwitz, S.B. *Pharmacol. Ther.* **1984**, *25*, 83. (d) Horwitz, S.B.; Lothstein, L.; Manfredi, J.J.; Mellado, W.; Parness, J.; Roy, S.N.; Schiff, P.B.; Sorbara, L.; Zeheb, R. *Ann. N. Y. Acad. Sci.* **1986**, *466*, 733. (e) Horwitz, S.B.; Schiff, P.B.; Parness, J.; Manfredi, J.J.; Mellado, W.; Roy, S.N. In *The Cytoskeleton*; Clarkson, T.W., Sager, P.R., Syversen, T.L.M., Eds.; Plenum: 1986. (f) Rowinsky, E.K.; Casenave, L.A.; Donehower, R.C. *J. Natl. Cancer Inst.* **1990**, *82*, 1247.
5. (a) Lavelle, F.; Fizames, C.; Guéritte-Voegelein, F.; Guénard, D.; Potier, P. *Proc. Am. Assoc. Cancer Res.* **1989**, *30*, 2254. (b) Bissery, M.C.; Guénard, D.; Guéritte-Voegelein, F.; Lavelle, F. *Cancer Res.***1991**, *51*, 4845.

6. Rao, S.; Horwitz, S.B.; Ringel, I. *J. Natl. Cancer Inst.* **1992**, *84*, 785.

7. Swindell, C.S.; Krauss, N.E.; Horwitz, S.B.; Ringel, I. *J. Med. Chem.* **1991**, *34*, 1176.

8. (a) Chmurny, G.N.; Hilton, B.D.; Brobst, S.; Look, S.A.; Witherup, K.M.; Beutler, J.A. *J. Nat. Prod.* **1992**, *55*, 414. (b) Baker, J.K. *Spectrosc. Lett.* **1992**, *25*, 31. (c) Falzone, C.J.; Benesi, A.J.; Lecomte, J.T.J. *Tetrahedron Lett.* **1992**, *33*, 1169. (d) Hilton, B.D.; Chmurny, G.N.; Muschik, G.M. *J. Nat. Prod.* **1992**, *55*, 1157.

9. Guéritte-Voegelein, F.; Guénard, F.; Mangatal, L.; Potier, P.; Guilhem, J.; Cesario, M.; Pascard, C. *Acta Cryst.* **1990**, *C46*, 781.

10. Peterson, J.R.; Do, H.D.; Rogers, R.D. *Pharmaceut. Res.* **1991**, *8*, 908.

11. Miller, R.W.; Powell, R.G.; Smith, Jr., C.R.; Arnold, E.; Clardy, J. *J. Org. Chem.* **1981**, *46*, 1469.

12. (a) Denis, J.-N.; Greene, A.E.; Serra, A.A.; Luche, J.-M. *J. Org. Chem.* **1986**, *51*, 46. (b) Denis, J.-N.; Correa, A.; Greene, A.E. *J. Org. Chem.* **1990**, *55*, 1957. (c) Ojima, I.; Habus, I.; Zhao, M.; Georg, G.I.; Jayasinghe, L.R. *J. Org. Chem.* **1991**, *26*, 1681. (d) Denis, J.-N.; Correa, A.; Greene, A.E. *J. Org. Chem.* **1991**, *56*, 6939. (e) Holton, R.A. U.S. Patent US 5 015 744, 1991; *Chem. Abstr.* **1992**, *115*, 159485b. (f) Deng, L.; Jacobsen, E.N. *J. Org. Chem.* **1992**, *57*, 4320.

13. (a) see for example : Sonntag, *Chem. Rev.* **1953**, *52*, 237; *Organic Synthesis I*, 99. (b) *^{1}H-NMR data* ($CHCl_3$; b = broad, d = doublet, t = triplet, m = multiplet) : **A** (δ, ppm) : 7.71 (o-NHBz, 2H, dd, J=7.5, 1.3 Hz); 7.41 (p-NHBz, 1H, tt, J=7.6, 1.3 Hz); 7.33 (m-NHBz, 2H, m); 7.27, 7.26 (o,m-Ph, together 4H); 7.21 (p-Ph, 1H, m); 6.5 (NH, 1H, b); 4.55 (CH_2, 2H, d, J=5.6 Hz). **B** (δ, ppm) : 7.95 (o-OBz, 2H, dd, J=8.0, 0.9 Hz); 7.69 (o-NHBz, 2H, dd, J=7.2, 1.1 Hz); 7.48 (p-OBz, 1H, tt, J=7.0, 0.9 Hz); 7.40 (p-NHBz, 1H, tt, J=7.6, 1.1 Hz); 7.35 (m-OBz, m), 7.33 (m-NHBz, m), together 4H; 6.40 (NH, 1H, d, J=8.3 Hz); 4.45 (CH^aH^bOBz, 1H, dd, J=10.6, 5.5 Hz). 4.39 (NHCH, 1H, m); 4.35 (CH^aH^bOBz, 1H, dd, J=10.6, 3.6 Hz); 1.65 (CH_2CH_3, 2H, m); 0.98 (CH_2CH_3, 3H, t, J=7.5 Hz). **C** (δ, ppm) : 7.66 (o-NHBz, 2H, dd, J=7.2, 1.1 Hz); 7.35 p-NHBz, 1H, tt, J=7.6, 1.1 Hz); 7.25 (m-NHBz, 2H, m); 6.80 (NH, 1H, d, J=8.1 Hz); 3.94 (NHCH, 1H, bm); 3.63 (CH^aH^bOH, 1H, dd, J=11.1, 3.6 Hz); 3.57 (CH^aH^bOH, 1H, dd, J=11.1, 5.6 Hz); 1.55 (CH_2CH_3, 2H, m); 0.86 (CH_2CH_3, 3H, t, J=7.4 Hz).

14. Saunders, M.; Houk, K.N.; Wu, Y.-D.; Still, W.C.; Lipton, M.; Chang, G.; Guida, W.C. *J. Am. Chem. Soc.* **1990**, *112*, 1419.

15. Mohamadi, F.; Richards, N.G.J.; Guida, W.C.; Liskamp, R.; Lipton, M.; Caufield, C.; Chang, G.; Hendrickson, T.; Still, W.C. *J. Comput. Chem.* **1990**, *11*, 440.

16. (a) Allinger, N.L. *J. Am. Chem. Soc.* **1977**, *99*, 8127. (b) Sprague, J.T.; Tai, J.C.; Yuh, Y.; Allinger, N.L. *J. Comput. Chem.* **1987**, *8*, 581. (c) Liljefors, T.; Tai, J.C.; Li, S.; Allinger, N.L. *J. Comput. Chem.* **1987**, *8*, 1051.

17. Still, W.C.; Tempczyk, A.; Hawley, R.C.; Hendrickson, T. *J. Am. Chem. Soc.* **1990**, *112*, 6127.

18. Chirlian, L.E.; Swindell, C.S.; Francl, M.M., in preparation. E-mail requests for generated coordinates should be addressed to cswindel@cc.brynmawr.edu.

19. Gigante, D.M.; Freedman, T.B.; Swindell, C.S.; Chirlian, L.E.; Francl, M.M.; Heerding, J.M.; Krauss, N.E., in preparation.

20. However, see ref. 8 and Guéritte-Voegelein, F.; Guénard, D.; Lavelle, F.; Le Goff, M-T.; Mangatal, L.; Potier, P. *J. Med. Chem.* **1991**, *34*, 992.